

# Absorption of Carbon Dioxide in Aqueous Piperazine/Methyldiethanolamine

Sanjay Bishnoi and Gary T. Rochelle

Dept. of Chemical Engineering, The University of Texas at Austin, Austin, TX 78712

*Carbon dioxide absorption in 0.6 M piperazine (PZ)/4 M methyldiethanolamine (MDEA) was measured in a wetted wall contactor. The data were simulated using a model that accounts for chemical reactions and transport effects with the eddy diffusivity theory. PZ/MDEA blends absorb CO<sub>2</sub> faster than monoethanolamine (MEA) or diethanolamine (DEA) blends with MDEA at similar concentrations. The reaction of PZ to form a monocarbamate is dominant at low loading (<0.14). The reaction of the monocarbamate to form dicarbamate is dominant at high loading. The absorption rate did not follow pseudo first-order behavior except at very low loading. All carbamate and dicarbamate formation reactions approached instantaneous behavior at high loading. The series resistance due to pseudo first-order reaction and instantaneous carbamate formation matched data throughout the entire loading range. A typical ammonia plant absorber was simulated at isothermal conditions using the rigorous model. Gas film limitations were dominant (>50%) only at the top of the absorber.*

## Introduction

The BASF corporation has commercialized activated methyldiethanolamine (MDEA) solvents with up to 0.8 M piperazine in 1.5 to 4.5 M MDEA (Appl et al., 1982). These solvents are widely used in the removal of carbon dioxide from synthesis gas in ammonia plants and hydrogen/carbon monoxide plants (Wammes et al., 1994). The popularity of these solvents appears to be due to the very fast kinetics (Bishnoi and Rochelle, 2000) which enables PZ to be added in very low concentrations. However, fundamental data on the PZ/MDEA/H<sub>2</sub>O/CO<sub>2</sub> system are very limited.

Bishnoi and Rochelle (2002) present data and a model of CO<sub>2</sub> solubility and piperazine speciation with MDEA/PZ blends. Data have been obtained at CO<sub>2</sub> loading (a measurement of CO<sub>2</sub> concentration in the liquid defined as moles of CO<sub>2</sub> per mole of total amine) from 0.005 to 0.2 in solutions of 0.6M PZ/4M MDEA at 313 to 343 K. In this loading region, PZ species make a significant difference on the partial pressure and information can be obtained about speciation at low loading. The electrolyte NRTL model was adjusted to match partial pressure data in the blended amine system at

low loading and concentrations determined from NMR data at high loading. The VLE measurements of Xu et al. (1998) and Liu et al. (1999) were evaluated by Bishnoi and Rochelle (2002). Unfortunately, these data have not been acquired in a region where there is any significant deviation from the behavior of MDEA.

Bishnoi and Rochelle (2000) studied the aqueous PZ system and showed that the rate constant of PZ with CO<sub>2</sub> is an order of magnitude higher than that of conventional carbamate formers such as monoethanolamine (MEA). Their studies on equilibrium partial pressure and NMR have shown that the second nitrogen on PZ is reactive to form protonated PZ carbamate and PZ dicarbamate. The pH of these systems, however, is never low enough to observe di-protonated PZ.

Xu et al. (1992) studied the absorption of CO<sub>2</sub> from gas at ambient pressures into aqueous blends of PZ/MDEA. The work of Xu et al. was performed at conditions where PZ was almost completely depleted at the gas/liquid interface and, therefore, no information can be gained about the kinetics of CO<sub>2</sub> with PZ (Bishnoi and Rochelle, 2000).

We now combine knowledge of the single amine systems (PZ/H<sub>2</sub>O/CO<sub>2</sub>) and (MDEA/H<sub>2</sub>O/CO<sub>2</sub>) with knowledge of the thermodynamics of the blended amine system to study the rate of absorption of CO<sub>2</sub> into PZ/MDEA blends. We

Correspondence concerning this article should be addressed to G. T. Rochelle.  
Current address of S. Bishnoi: The El Paso Corp., 1001 Louisiana St., Houston, TX 77002.

specifically target experiments where the total CO<sub>2</sub> concentration is less than the total PZ concentration and driving forces where PZ is not depleted at the interface. The apparent second-order rate constant of PZ/CO<sub>2</sub> is seen to double in the presence of 4M MDEA, leading us to believe that MDEA participates in the reaction of PZ with CO<sub>2</sub>. This is consistent with the zwitterion mechanism proposed for DEA and other secondary amines (Caplow, 1968). Measurements are also made at loading, partial pressure, and temperature representative of industrial absorption.

A new rigorous model for calculating the concentration gradients of all species throughout the boundary layer and the enhancement factor for CO<sub>2</sub> absorption is presented. The new model is based largely on Glasscock (1990) who showed that the eddy diffusivity theory is equivalent to the penetration theory or surface renewal theory. The resulting rate-based model is combined with the thermodynamics model of Bishnoi and Rochelle (2002) to make predictions of the rate of absorption, enhancement factor, and height and volume of the transfer unit at industrially significant conditions. These results are presented and compared to other promoted MDEA systems.

## Model Description

Eddy diffusivity theory is used in this work. Glasscock and Rochelle (1989) demonstrated that eddy diffusivity theory was effective for modeling acid gas absorption by amines. They showed that the predicted absorption rate never deviates more than 3% from surface renewal theory predictions at conditions indicative of CO<sub>2</sub> absorption with amines.

For absorption of CO<sub>2</sub> into a nonreactive solvent, Glasscock and Rochelle used the following expression to represent the material balance of CO<sub>2</sub> in the liquid where  $x$  represents the liquid depth away from the gas-liquid interface

$$\frac{d}{dx} \left[ (D_{\text{CO}_2} + \epsilon x^m) \frac{d}{dx} [\text{CO}_2] \right] = 0 \quad (1)$$

Close to the interface ( $x = 0$ ), mass transfer is dominated by the diffusion coefficient of CO<sub>2</sub>. As  $x$  increases (toward the bulk solution), the effect of eddies becomes more important.

This expression excludes the effect of electrical potential on ion diffusion, which Glasscock and Rochelle show to be insignificant for promoted amine systems. By making this simplifying assumption, we must assume all ion diffusion coefficients to be equal. We use a value of 2 for  $m$ . This value is suggested by Prasher and Fricke (1974) and is consistent with the work of Glasscock. The mass-transfer coefficient then becomes

$$k'_{i,\text{CO}_2} = \frac{2}{\pi} \sqrt{\epsilon D_{\text{CO}_2}} \quad (2)$$

The integration is performed to infinite value of  $x$ . In order to deal with the integration numerically, we must perform a variable transformation such that the upper bound is finite. This work uses the space variable transformation used in the work of Glasscock, originally proposed by Versteeg (1987)

$$r = \frac{2}{\pi} \tan^{-1} \left( x \sqrt{\frac{\epsilon}{D}} \right) \quad (3)$$

This dimensionless transformation is helpful in the numerical solution since it bounds the space variable and results in a linear concentration gradient for physical mass transfer.

We divide the  $r$  space from 0 to 1 into 38 nodes (starting at the gas liquid interface and moving into the liquid phase: 1 node at  $r = 0$ , 10 nodes with grid spacing of 1.0 E-4, 9 nodes with grid spacing of 1.0 E-3, 9 nodes with grid spacing of 1.0 E-2, 9 nodes with grid spacing of 0.1). Three point forward differencing was used at the interface to describe all derivatives

$$\left( \frac{df}{dr} \right)_i = \frac{1}{2\Delta r} (-3f_i + 4f_{i+1} - f_{i+2}) \quad (4)$$

Three point central difference formulas were used where there were equal grid sizes on each side of the node of interest

$$\left( \frac{df}{dr} \right)_i = \frac{1}{2\Delta r} (-f_{i-1} + f_{i+1}) \quad (5)$$

$$\left( \frac{d^2f}{dr^2} \right)_i = \frac{1}{(\Delta r)^2} (f_{i-1} - 2f_i + f_{i+1}) \quad (6)$$

The finite difference scheme for nonuniform grid size of Liu et al. (1994) was used at nodes where the grid size changed.

The material balance equations are derived and presented in Appendix E of Bishnoi (2000). In  $x$  space we can express the material balance in the following form

$$\nabla((Di + \epsilon x^2)\nabla[i]) = -\mathcal{R}_i \quad (7)$$

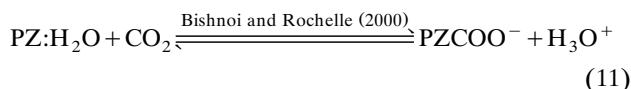
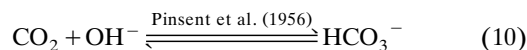
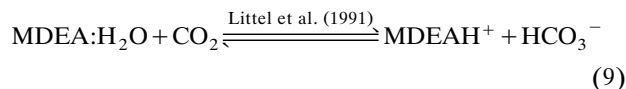
where  $i$  is a component to be included in the model,  $\epsilon$  is the mass transfer coefficient parameter,  $\mathcal{R}_i$  is the overall rate of the reaction of species  $i$ , and  $\nabla$  is the derivative operator with respect to the space variable  $x$ .

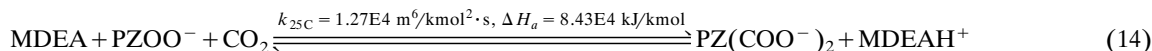
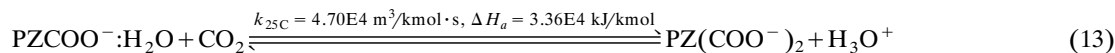
We simplify this further as

$$\nabla^2[i] = -\mathcal{R}_i \quad (8)$$

where  $\nabla^2$  can be considered the Eddy Diffusivity operator.

A proper understanding of the model used in this work begins with a discussion of all species and reactions used. The following six reactions are assumed to be kinetically controlled and reversible





For example, the rate of MDEA reaction with  $\text{CO}_2$  is given by

$$R_9 = k_{\text{MDEA}} \left( [\text{MDEA}][\text{CO}_2] - \frac{[\text{MDEAH}^+][\text{HCO}_3^-]}{K_9} \right) \quad (15)$$

where  $k_{\text{MDEA}}$  is given by

$$k_2 = k_{25\text{C}} \cdot \exp \left[ -\frac{\Delta H_a}{R} \left( \frac{1}{T} - \frac{1}{298.15} \right) \right] \quad (16)$$

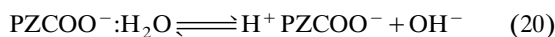
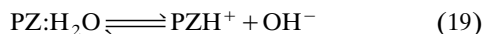
and the equilibrium constant

$$K_9 = \frac{[\text{MDEAH}^+][\text{HCO}_3^-]}{[\text{MDEA}][\text{CO}_2]}$$

and is calculated by the ratio of the species in the bulk solution.

Note that water is left out of the kinetic and equilibrium expressions since it is considered to be constant across the boundary layer and, therefore, can be lumped with the apparent rate and equilibrium constants.

Reactions involving only a proton transfer are always considered to be in equilibrium. All equilibrium constants are calculated directly from the ratio of products and reactants in the bulk solution. Since the bulk solution is speciated using the equilibrium model of Bishnoi and Rochelle (2002), the equilibrium constants used in this work are consistent with that work. These reactions are



The equations to be solved at each node are presented in Table 1. Along with these 11 equations at each node, we define boundary conditions at the interface and in the bulk solution. We use the condition that all concentrations are equal to the equilibrium concentrations as liquid depth approaches infinity ( $x = \infty$ ,  $r = 1$ ). We also assume phase equilibrium of  $\text{CO}_2$  at the interface leading to a known concentration of  $\text{CO}_2$  at the interface for a given interfacial partial pressure of  $\text{CO}_2$ . The concentration of species which undergo proton exchange are defined by the combined buffer system flux being zero at the interface and chemical equilibrium between the two species involved in the proton exchange. Since dicarba-

mate does not go through a rapid proton exchange, its flux is considered to be zero at the interface. Electroneutrality is also assumed at the interface. Table 1 also documents the boundary conditions used in this work.

**Table 1. Model Equations and Boundary Conditions**

<b>Conservation Equations at Each Node</b>	
<i>Overall Species Material Balance</i>	
$\nabla^2[\text{PZ}] + \nabla^2[\text{PZCOO}^-] + \nabla^2[\text{H}^+ \text{PZCOO}^-] + \nabla^2[\text{PZH}^+] + \nabla^2[\text{PZ}(\text{COO}^-)_2] = 0$	
$\nabla^2[\text{MDEA}] + \nabla^2[\text{MDEAH}^+] = 0$	
$\nabla^2[\text{CO}_2] + \nabla^2[\text{HCO}_3^-] + \nabla^2[\text{CO}_3^{=}] + \nabla^2[\text{PZCOO}^-] + \nabla^2[\text{H}^+ \text{PZCOO}^-] + 2\nabla^2[\text{PZ}(\text{COO}^-)_2] = 0$	
<i>Equilibrium Relationships</i>	
$K_{18} = \frac{[\text{MDEAH}^+][\text{OH}^-]}{[\text{MDEA}]}$	
$K_{19} = \frac{[\text{PZH}^+][\text{OH}^-]}{[\text{PZ}]}$	
$K_{20} = \frac{[\text{H}^+ \text{PZCOO}^-][\text{OH}^-]}{[\text{PZCOO}^-]}$	
$K_{17} = \frac{[\text{CO}_3^{=}]}{[\text{HCO}_3^-][\text{OH}^-]}$	
<i>Material Balance for Molecular CO<sub>2</sub></i>	
$\nabla^2[\text{CO}_2] - (R_9 + R_{10} + R_{11} + R_{12} + R_{13} + R_{14}) = 0$	
<i>Carbamate Buffer System Balance</i>	
$\nabla^2[\text{PZCOO}^-] + \nabla^2[\text{H}^+ \text{PZCOO}^-] + R_{11} + R_{12} - (R_{13} + R_{14}) = 0$	
<i>Dicarbamate Material Balance</i>	
$\nabla^2[\text{PZ}(\text{COO}^-)_2] + R_{13} + R_{14} = 0$	
<i>Electroneutrality</i>	
$[\text{MDEAH}^+] + [\text{PZH}^+] = [\text{HCO}_3^-] + 2[\text{CO}_3^{=}] + [\text{OH}^-] + [\text{PZCOO}^-] + 2[\text{PZ}(\text{COO}^-)_2]$	
<b>Boundary Conditions</b>	
<i>At <math>x = 0</math></i>	
$[\text{CO}_2] = [\text{CO}_2]_i$	
$D_{\text{PZ}}\nabla[\text{PZ}] + D_{\text{PZH}^+}\nabla[\text{PZH}^+] = 0$	
$K_{19}[\text{PZ}] - [\text{PZH}^+][\text{OH}^-] = 0$	
$D_{\text{MDEA}}\nabla[\text{MDEA}] + D_{\text{MDEAH}^+}\nabla[\text{MDEAH}^+] = 0$	
$K_{18}[\text{MDEA}] - [\text{MDEAH}^+][\text{OH}^-] = 0$	
$D_{\text{PZCOO}^-}\nabla[\text{PZCOO}^-] + D_{\text{H}^+ \text{PZCOO}^-}\nabla[\text{H}^+ \text{PZCOO}^-] = 0$	
$K_{20}[\text{PZCOO}^-] - [\text{H}^+ \text{PZCOO}^-][\text{OH}^-] = 0$	
$D_{\text{HCO}_3^-}\nabla[\text{HCO}_3^-] + D_{\text{CO}_3^{=}}\nabla[\text{CO}_3^{=}] = 0$	
$K_{17}[\text{HCO}_3^-][\text{OH}^-] - [\text{CO}_3^{=}] = 0$	
$\nabla[\text{PZ}(\text{COO}^-)_2] = 0$	
$[\text{MDEAH}^+] + [\text{PZH}^+] = [\text{HCO}_3^-] + 2[\text{CO}_3^{=}] + [\text{OH}^-] + [\text{PZCOO}^-] + 2[\text{PZ}(\text{COO}^-)_2]$	
<i>At <math>x = \infty</math></i>	
$[i] = [i]_o$ For all species $i$ in solution	

**Table 2. Absorption of CO<sub>2</sub> into 0.6 M PZ, 4 M MDEA at Low Loading**

T (K)	Bulk Gas P <sub>CO<sub>2</sub></sub> (Pa)	k <sub>g</sub> × 10 <sup>5</sup> (mol/atm · cm <sup>2</sup> · s)	k <sub>1</sub> × 10 <sup>5</sup> (m/s)	Loading CO <sub>2</sub> /mol Amine)	Flux × 10 <sup>8</sup> (mol/cm <sup>2</sup> · s)	
					Measured	Predicted (Rigorous)
295	151	2.84	1.83	0.0015	1.32 ± 0.11	1.30
295	207	2.87	1.82	0.0021	1.87 ± 0.15	1.78
295	261	2.90	1.82	0.0018	2.44 ± 0.20	2.27
295	290	2.89	1.83	0.0013	2.77 ± 0.22	2.51
313	15	2.86	2.36	0.0056	0.15 ± 0.01	0.16
313	169	2.89	2.06	0.0039	2.05 ± 0.16	2.10
313	212	2.90	2.47	0.0050	2.47 ± 0.20	2.64
313	252	2.91	2.06	0.0044	2.95 ± 0.24	3.15
313	276	2.95	2.07	0.0044	3.31 ± 0.26	3.45
343	127	3.02	5.38	0.0011	2.15 ± 0.17	2.17
343	188	3.06	5.30	0.0020	3.10 ± 0.25	2.89
343	224	3.14	5.42	0.0024	3.49 ± 0.28	3.39
343	243	3.17	5.32	0.0016	4.02 ± 0.32	3.88

G ≅ 5 SLPM, L ≅ 2 cc/s. See Bishnoi (2000).

### Physical Properties

The Henry's law constant for CO<sub>2</sub> (H<sub>CO<sub>2</sub></sub>) is obtained using the N<sub>2</sub>O analogy with the solubility of N<sub>2</sub>O measured in MDEA and correlated by Al-Ghawas et al. (1989)

$$H_{\text{CO}_2} = \frac{H_{\text{CO}_2, \text{H}_2\text{O}}}{H_{\text{N}_2\text{O}, \text{H}_2\text{O}}} \quad (21)$$

The diffusion coefficient of MDEA is obtained from correlation of the Rowley (1999) data reported in Bishnoi (2000).

Diffusion coefficients for PZ are calculated using the diffusion coefficient of MDEA corrected for molecular weight by multiplying by a factor of 1.2. Diffusion coefficients of all ions are arbitrarily set at the same value as PZ.

The diffusion coefficient of CO<sub>2</sub> in concentrated MDEA solutions is calculated using the N<sub>2</sub>O analogy with values of D<sub>N<sub>2</sub>O</sub> measured by Versteeg (1987). Pacheco (1998) presents a correlation for the diffusion coefficient of N<sub>2</sub>O in amine solution that takes the form of the Stokes-Einstein equation

$$D_{\text{N}_2\text{O}}(\text{cm}^2/\text{s}) = 5.33E - 8 \frac{T}{\mu^{0.545}} \quad (22)$$

Here, the solution viscosity is calculated using the correlation of Glasscock (1990).

We assume that the physical properties do not vary with solution loading.

### Experimental Methods

The absorption rate of carbon dioxide was determined in a wetted wall column. The use of this apparatus to provide data for CO<sub>2</sub> absorption in amine solutions has been described in detail by Bishnoi and Rochelle (2002) and Bishnoi (2000). Solution flowed down the outside of a stainless steel tube that was 9.1 cm long with a contact area of 38.52 cm<sup>2</sup>. The column operated at 1 to 8 atm with gas rates of 4 to 6 L/min. Loaded amine solution was recirculated at 2 cm<sup>3</sup>/s from reservoirs of 0.4 to 2.4 L volume.

The absorption rate was determined from continuous infrared analysis of the gas leaving the system. The reported CO<sub>2</sub> partial pressure is the log mean average of the gas entering and leaving the contactor.

The liquid film mass-transfer coefficient was determined by CO<sub>2</sub> desorption from water and ethylene glycol mixtures. The gas film coefficient was determined by the absorption of sulfur dioxide into sodium hydroxide solutions.

**Table 3. Absorption of CO<sub>2</sub> into Partially Loaded 0.6 M PZ, 4 M MDEA Solutions at Low Driving Force**

T (K)	Bulk Gas		k <sub>g</sub> × 10 <sup>5</sup> (mol/(atm · cm <sup>2</sup> · s))	k <sub>1</sub> × 10 <sup>5</sup> (m/s)	Loading (mol CO <sub>2</sub> /mol Amine)	Flux × 10 <sup>7</sup> (mol/cm <sup>2</sup> · s)	
	P <sub>CO<sub>2</sub></sub> (kPa)	P <sub>CO<sub>2</sub></sub> <sup>*</sup> (kPa)				Measured	Predicted (Rigorous)
313	5.25	0.36	1.43	2.87	0.095	3.61 ± 0.29	3.09
313	3.42	0.54	2.36	3.00	0.111	2.61 ± 0.21	2.07
313	3.47	0.76	2.36	2.87	0.125	2.43 ± 0.19	1.83
313	3.53	1.05	2.36	2.89	0.140	2.19 ± 0.18	1.52
313	4.29	1.31	2.88	2.89	0.151	0.96 ± 0.08	1.72
313	9.04	2.40	2.85	2.87	0.185	2.60 ± 0.21	2.85
313	14.4	4.26	2.29	2.84	0.225	3.33 ± 0.27	3.09
313	20.5	7.91	1.62	2.84	0.281	3.21 ± 0.26	2.61
313	27.3	10.33	1.19	2.87	0.311	4.02 ± 0.32	2.87
343	1.08	0.01	3.42	6.31	0.004	1.83 ± 0.15	1.41
343	2.32	0.09	3.42	6.19	0.013	3.47 ± 0.28	2.75
343	3.53	0.42	3.42	6.00	0.027	4.43 ± 0.35	3.10
343	4.44	0.81	3.44	6.14	0.038	5.02 ± 0.40	3.10

G ≅ 5 SLPM, L ≅ 2 cm<sup>3</sup>. (See Bishnoi (2000)).

**Table 4. Absorption of CO<sub>2</sub> into Partially Loaded 0.6 M PZ/4 M MDEA Solutions at High Driving Force and 313 K\***

Bulk Gas $P_{\text{CO}_2}$ (kPa)	$P_{\text{CO}_2}^*$ (kPa)	$k_g \times 10^6$ (mol/(atm· cm <sup>2</sup> ·s))	$k_1 \times 10^5$ (m/s)	Loading (mol CO <sub>2</sub> / mol Amine)	Flux $\times 10^6$ (mol/cm <sup>2</sup> ·s)	
					Measured	Predicted (Rigorous)
97	5.37	9.35	3.44	0.244	1.93 ± 0.97	1.23
100	7.68	9.23	3.43	0.278	1.70 ± 0.85	1.10
99	10.15	9.39	3.46	0.309	1.59 ± 0.80	1.00
103	12.48	9.13	3.49	0.335	1.43 ± 0.72	0.94
95	18.25	9.30	3.53	0.391	1.20 ± 0.60	0.74
100	17.47	9.04	3.46	0.384	1.07 ± 0.54	0.77
150	27.86	3.08	3.66	0.466	1.42 ± 0.71	0.76
156	31.99	3.03	3.49	0.493	1.27 ± 0.64	0.70
155	33.14	3.07	3.62	0.500	1.25 ± 0.63	0.70
165	40.14	3.04	3.63	0.539	0.95 ± 0.48	0.64
166	44.02	3.04	3.64	0.558	0.94 ± 0.47	0.61
167	49.46	3.03	3.67	0.582	0.91 ± 0.46	0.55
175	61.10	3.01	3.65	0.625	0.64 ± 0.32	0.46

\*See Kaganoi (1997).

### Experimental Data

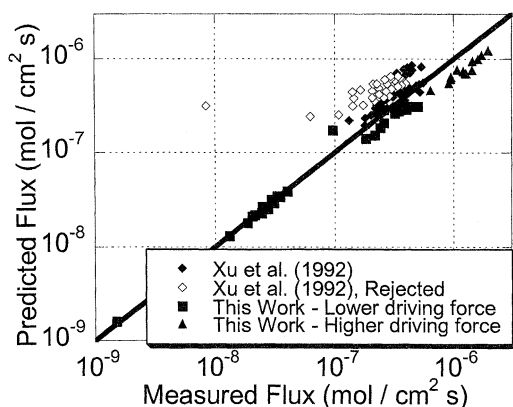
Experimental data obtained in this work are presented in Tables 2, 3 and 4 along with model predictions. A subset of the Xu data is shown in Figure 4 (details are given in Bishnoi, 2000). Model predictions of all the Xu data are shown in Figure 1. The model does a good job of fitting data over a wide range of measured fluxes as shown by the parity plot in Figure 1. The data of Xu et al. (1992) are divided into two subsets: accepted and rejected. The details of this will be discussed in a later section.

### Interpretation of data taken at low loading

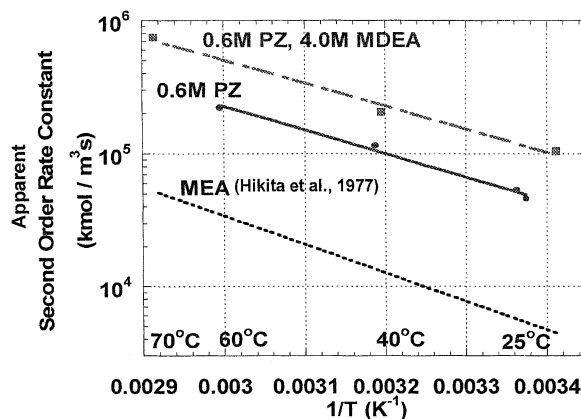
Table 2 shows data for the absorption of CO<sub>2</sub> into 0.6 M PZ, 4 M MDEA at low loading. The bulk phase partial pressure of CO<sub>2</sub> in this table is the log mean average of inlet and outlet pressures. At these conditions, the concentration of all ionic species is very low making all reactions except 11 and 12 unimportant. Since the concentration of all reaction products is low, we only need to consider the forward reactions at these conditions. As shown by Table 2, the model matches absorption data for CO<sub>2</sub> into unloaded solutions well.

Figure 2 shows the apparent second-order reaction of PZ with CO<sub>2</sub> for PZ alone and in the presence of 4 M MDEA. Each point represents several experimental partial pressures and the procedure of extracting the apparent second-order rate constant from the data shown in Table 2 has been described by Bishnoi and Rochelle (2000). The rate constant for reaction 11 was documented in that article as well. MDEA appears to participate in the reaction of CO<sub>2</sub> and PZ to form carbamate. This observation is consistent with the zwitterion mechanism, originally reported by Caplow (1968). The zwitterion mechanism has been observed in several other secondary amines (Danckwerts, 1979; Littel, 1991.)

Glasscock et al. (1991) showed that this effect can be modeled by including the participation of MDEA in carbamate formation (reaction 12). The third-order rate constant for this reaction was regressed to fit the absorption data at low loading and found to follow the Arrhenius expression presented in the second section. It should be noted that modeling the zwitterion mechanism as two parallel reactions (one with water deprotonation and one with MDEA deprotonation) assumes that the deprotonation by PZ is negligible. This appears to be true, based on the data presented by Bishnoi and



**Figure 1. Fit of the rigorous model to all PZ/MDEA adsorption data.**



**Figure 2. Comparison of CO<sub>2</sub> absorption into aqueous PZ, PZ/MDEA blend, and MEA.**

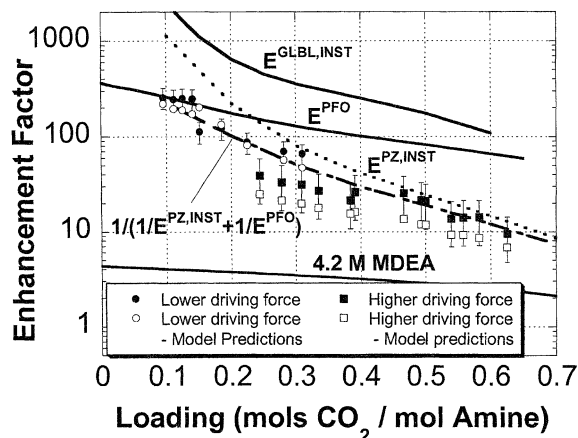


Figure 3. Enhancement factors for 0.6 M PZ/4 M MDEA at 40°C and  $k_1^o = 3.3E-5$  m/s.

Rochelle (2000) where there was no effective change in the second-order rate constant of PZ in 0.2 M solutions and 0.6 M solutions. We would expect the deprotonation by PZ to be as fast as the deprotonation by MDEA, however, we can ignore the PZ reaction because its low concentration never allows it to dominate. In the aqueous system, the deprotonation of the zwitterion by water to form hydronium ion will dominate.

#### Data taken in loaded solutions

*Data Taken in this Work.* Table 3 shows the absorption measurements taken in this work and model predictions in loaded solutions of PZ/MDEA. We have included a finite rate for the formation of PZ dicarbamate from PZ monocarbamate (reactions 13 and 14). Without the inclusion of reactions 13 and 14, the data taken in loaded solutions was always underpredicted (40% lower than current model predictions). The sensitivity of the predicted flux to the rate con-

stant for reactions 13, however, is low requiring us to adjust it manually. The rate constant for reaction 14 is set by assuming the same ratio for the rate constant of 14 to 13 as 12 to 11. This assumes that the effect of MDEA on the reaction of PZ with  $CO_2$  is the same as the effect of MDEA on the reaction of  $PZCOO^-$  with  $CO_2$ .

Figure 3 compares measured enhancement factor and predictions from several simple models. The solid points represent experimental data, while the open points represent the model predictions.

The pseudo first-order model (Danckwerts, 1979; shown in Eq. 23) is a good assumption for MDEA solutions since the reaction of MDEA is slow enough that no significant depletion of MDEA occurs at the interface. The pseudo first-order curve for the blend matches the data only at low loading. However, it is not a good assumption for PZ/MDEA blends at the practical conditions of the data taken in loaded solutions in this work

$$E^{PFO} = \sqrt{\frac{(\sum k_{Am}[Am]) D_{CO_2}}{k_i^2}} \quad (23)$$

The enhancement factor predicted by the simple model of instantaneous reactions and small driving force (derived in Bishnoi, 2000;  $E^{GLBL,INST}$ ) is also not a good approximation of the data

$$E^{GLBL,INST} = \frac{k^o l, PROD [Am]_T H_{CO_2}}{k_{i,CO_2}^o \frac{\partial P_{CO_2}^*}{\partial \alpha}} \quad (24)$$

A good approximation is obtained at high loading if we only consider the PZ reactions to be instantaneous by increasing all carbamate and dicarbamate formation rate constants to very large numbers ( $E^{PZ,INST}$ ). The dashed line in Figure 3 is the combined enhancement factor for pseudo first order with instantaneous PZ reactions defined by Eq. 25. A derivation of Eqs. 24 and 25 can be found in Bishnoi (2000)

$$E = \left( \frac{1}{\frac{1}{E^{PZ,INST}} + \frac{1}{E^{PFO}}} \right) \quad (25)$$

In the rigorous model, the second-order rate constant for piperazine carbamate and  $CO_2$  to form piperazine dicarbamate (reaction 13) was adjusted and found to be 90,000 L/mol·s at 40°C. This is lower than the rate constant of piperazine to form piperazine carbamate (reaction 11), which was found by Bishnoi and Rochelle (2000) to be 102,000 L/mol·s. This is consistent with the Bronsted theory, which suggests a decrease in carbamate formation rate with a decrease in amine  $pK_a$ . We believe we have found a higher value for the reaction 13 rate constant than the Bronsted theory would suggest (around 60,000 L/mol·s) since it is the only parameter adjusted to match the high loading data. It, therefore, encompasses many other charges as the solution is loaded with  $CO_2$ .

The gas-phase partial pressure of  $CO_2$  in the experimental data taken here are 5 to 6 times above the value in equilibrium with the liquid phase. The presence of 0.6 M PZ en-

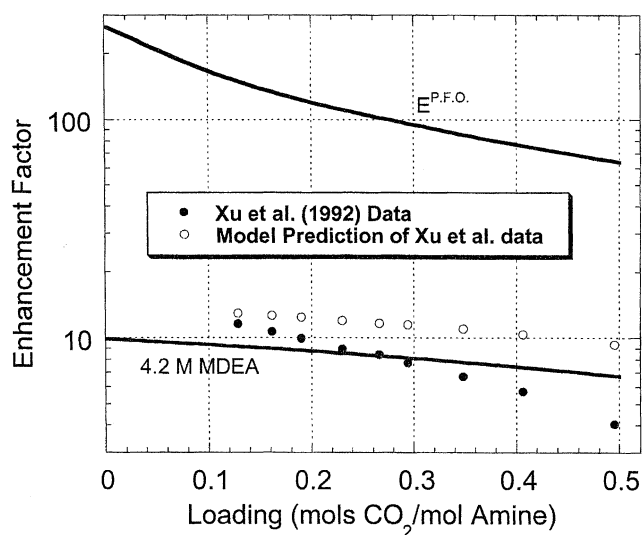


Figure 4. Enhancement factors for 0.1 M PZ/4.21 M MDEA at 40°C and  $k_1^o = 2E-5$  m/s.

hances the rate of removal above that of 4M MDEA by almost two orders of magnitude at moderate loading (<0.15) and up to an order of magnitude at high loading (<0.3).

*Data Taken in Loaded Solutions with High Driving Force.* We analyze CO<sub>2</sub> absorption rates in 0.6M PZ/4M MDEA at 40°C with high driving force (data of Kaganoi (1997)). Data and model predictions are shown in Table 4. The gas side bulk phase partial pressures of CO<sub>2</sub> studied in this section are up to 2 atm.

The model presented in this work consistently underpredicts Kaganoi's data by 30–40%. No further parameters were adjusted, however, to match this data. This is because no parameters were found to make a significant difference in the model fit of the data, within reasonable changes of the parameters. The sensitivity of the model prediction of flux to the important parameters is discussed in Figure 6. There are two explanations for the discrepancy of the model predictions and the measured values.

(1) There is a possibility that the discrepancy between the model prediction and the data could be an experimental error. For this subset of data, the percent removal of CO<sub>2</sub> across the wetted wall contactor is only about 15–20%. This means that the flux is calculated by taking the difference of two large numbers and can lead to large errors. A combined error of 5% in reading the partial pressure in and out of the contactor can result in a 25% error in the flux. Also, error in the driving force due to uncertainty in the equilibrium partial pressure could result in an error of up to 50% in the enhancement factor at Kaganoi's experimental conditions. All of this data was taken in two experiments where it appears that the amine solution and analyzer calibrations were not changed from one run to the next, leading us to believe the error could be systematic.

(2) The model does not account for the direct reaction of MDEA with carbamate species. With Table 6, we show that carbamate reversion to CO<sub>2</sub> and the subsequent reaction of the freed CO<sub>2</sub> with MDEA occurs, but is never significant. There is possibly a direct reaction of carbamate with MDEA which makes absorption faster than predicted in this work. We recommend experimental investigation of this phenomenon by keeping the loading of the solution constant and varying the driving force. If there is a direct interaction of the carbamate with MDEA, the model prediction of the flux will increasingly underpredict the measured flux with increasing driving force.

The high driving force data is also shown in Figure 3. Even at these conditions, it appears as though 0.6 M PZ results in a significant enhancement above the performance of 4M MDEA.

Once again, the assumption of instantaneous reactions with small driving forces or pseudo first-order behavior would result in a very large error of the predicted enhancement factor. The combination of instantaneous PZ reactions with pseudo first order does an adequate job of modeling the data ( $1E^{PZ,INST} + 1/E^{PFO}$ ). The rigorous model does an adequate job of predicting the measured flux.

*Data of Xu et al. (1992).* Xu et al. (1992) measured absorption of pure CO<sub>2</sub> (1 atm) in MDEA solutions with 0.04 to 0.2 M PZ. Unfortunately, the measured enhancement was not significantly different from enhancement in MDEA solutions making it impossible to gain any information about the effect of PZ. This is shown in Figure 4, which examines a subset of the Xu et al. (1992) data at 40°C and 0.1 M PZ, 4.21 M MDEA. This shows that the data of Xu et al. is best described as pseudo-first-order absorption into unpromoted MDEA. They have measured the flux by taking the difference of outlet and inlet gas-flow rates. Since absorption is small, their flux measurements may be prone to large errors. Details of their data and our model predictions of their data are shown in Appendix D of Bishnoi (2000).

Figure 4 also demonstrates the experimental error of the Xu et al. data. It is unreasonable to expect that PZ has a negative effect on the enhancement factor, yet this is what the data above a loading of 0.3 seems to suggest. Furthermore, one of the published points predicts an enhancement factor of 0.3, which is unreasonable. The data set of Xu et al., therefore, is divided into two sets: accepted points (those that lie above the MDEA curve) and rejected points (those that lie below).

*Model Predictions for the Single Amine Systems.* The data presented by Bishnoi and Rochelle (2000) for CO<sub>2</sub> absorption into aqueous PZ have been reinterpreted using the rigorous model (Table 5). As can be seen, the inclusion of the PZ carbamate rate constant has improved the model predictions to within 10%, showing that the model can be used in the limit of no MDEA.

*Model Predictions.* The model developed in this work has been used to generate insight as to how PZ activated MDEA blends derive their effectiveness. We present a comparison of PZ/MDEA blends to other promoted systems (MEA/MDEA and DEA/MDEA). The relative sensitivity of model parameters is also shown along with predictions that show what the important reactions are at different conditions. The specific case of ammonia plants is also discussed.

*Comparison with other Promoters.* Figure 5 compares the effectiveness of PZ/MDEA blends with DEA/MDEA and MEA/MDEA blends. Results are compared to pseudo-first-order predictions for MDEA. The MEA and DEA blend calculations are from the work of Glasscock et al. (1991). We

**Table 5. Model Predictions of CO<sub>2</sub> Absorption into 0.6 M PZ at 313 K (data of Bishnoi and Rochelle, 2002)**

Bulk Gas $P_{CO_2}$ (Pa)	$k_g \times 10^5$ (mol/(atm·cm <sup>2</sup> ·s))	$k_1 \times 10^4$ (m/s)	Loading (mol CO <sub>2</sub> / mol Amine)	Flux × 10 <sup>7</sup> (mol/cm <sup>2</sup> ·s)		
				Measured	Previous Prediction*	Predicted (Rigorous)
2,208	2.11	1.11	0.29	2.39 ± 0.19	2.19	2.18
2,207	2.02	1.10	0.47	2.14 ± 0.17	1.60	1.81
2,470	2.18	1.12	0.56	1.88 ± 0.15	1.52	1.79
2,600	2.11	1.11	0.67	1.47 ± 0.12	1.02	1.29

\*Predictions of Bishnoi and Rochelle (2000) which exclude PZCOO<sup>-</sup> kinetics.

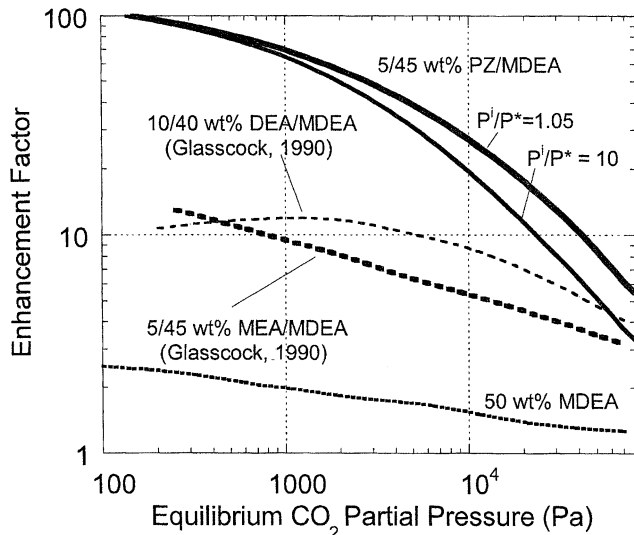


**Figure 5. Comparison of PZ/MDEA blends to conventional blends.**

Predictions at 40°C,  $k_1^o = 1.0E-4$  m/s.  $P^i/P^* = 1.05$  unless specified.

see that the PZ blend enhances the performance of MDEA by a factor of 50 at low loading. Even at high loading (0.5 mol  $CO_2$ /mol amine;  $P_{CO_2}^* = 33$  kPa), the PZ blend can be up to a factor of 5 more effective than 50% MDEA.

PZ is found to be a more effective promoter than MEA or DEA, especially at low loading. The high driving force is not seen to have a major effect on the predicted enhancement factor except at high loading. The decrease in enhancement is due to the depletion of PZ and PZ carbamate at the interface.

**Sensitivity to Model Parameters.** Figure 6 shows the sensitivity of the calculated flux to several parameters using 5 wt. % PZ/45 wt. % MDEA at 313 K. The rate constant for PZ and MDEA catalyzed PZ (reactions 11 and 12) are lumped into one parameter, as are the rate constants for  $PZCOO^-$  and  $PZCOO^-$  catalyzed with MDEA (reactions 13 and 14). The diffusion coefficients of MDEA, PZ, and ions are also studied.

The results can be divided into three regions. In the first region, where the concentration of  $CO_2$  is lower than the

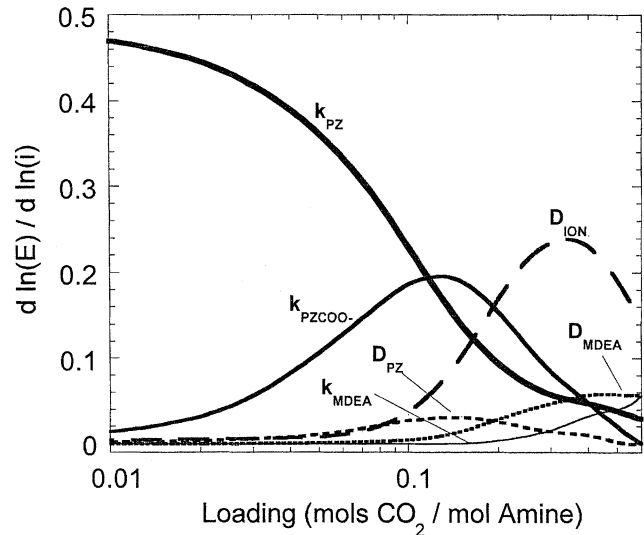


**Figure 6. Model sensitivity to rate and mass-transfer parameters.**

Predictions in 5/45 wt. % PZ/MDEA at 40°C and  $k_1^o = 1.0E-4$  m/s.

total concentration of PZ (loading < 0.13), the rate constant of PZ is by far the most sensitive parameter showing that the dominant phenomenon is still the direct reaction of  $CO_2$  with PZ. In the second region, where the total concentration of  $CO_2$  is lower than two times the concentration of PZ (loading < 0.26), the rate constant of PZ carbamate becomes the most sensitive parameter (region 2). In the third region, where the total concentration of  $CO_2$  is higher than two times the total concentration of PZ, the most sensitive parameter is the diffusion coefficient of ions showing that the removal of reaction products has become the dominant phenomenon. Another interesting result is that the rate constant of MDEA is not more sensitive than the rate constant of PZ or PZ carbamate until a loading of around 0.4.

**Reaction Zones and Deviation from Approximate Solutions.** Table 6 shows model predictions of the enhancement factor of  $CO_2$  absorption into 0.6 M/4 M blend of PZ/MDEA at 313 K and a  $k_1^o = 1.0E-4$  m/s. A series of driving force conditions varying from a low driving force ( $1.05^*P_{CO_2}^*$ ) to a high

**Table 6. Enhancement Factors for 0.6 M PZ, 4 M MDEA at 313 K and Various Driving Force**

Loading	$P_{CO_2}^*$ (Pa)	$E^{P.F.O.}$	$E^{1.05P^*}$	$E^{Series}$	$E^{2P^*}$	$E^{5P^*}$	$E^{10P^*}$	$E^{PZ,INST}$	$E^{GLPL,INST}$
0.01	5	123.9	121.9		121.8	121.8	121.7		26,600
0.02	17	118.4	115.8		115.7	115.6	115.4		
0.05	82	110.6	106.9	106.9	106.7	106.2	105.4	3214	7,840
0.07	167	103.3	98.5		98.2	97.2	95.6		4,810
0.10	404	92.4	85.5	85.8	84.8	82.8	79.7	1194	2,480
0.15	1,272	75.7	64.8	65.2	63.4	59.3	53.5	469	1,120
0.20	2,991	62.7	48.4	49.5	46.3	40.7	34.0	235	647
0.25	5,685	53.1	36.5	37.5	34.0	28.1	22.0	128	451
0.30	9,309	46.0	28.0	29.3	25.5	20.0	15.0	81	356
0.40	19,099	36.0	17.8	18.9	15.5	11.4	8.2	40	252
0.50	25,400	29.0	11.8	12.8	10.0	7.2	5.2	23	176
0.60	32,800	23.3	7.8		6.6	4.7	3.5		109
0.70	89,700	18.2	5.0		4.2	3.1	2.4		

$$1/E^{series} = (1/E^{PFO} + 1/E^{PZ,INST})^{-1}$$

**Table 7. Concentrations and Approach to Equilibrium for CO<sub>2</sub> Absorption into 5/45 wt. % PZ/MDEA at 313 K\***

Parameter	0.07		0.2		0.65	
	mol CO <sub>2</sub> /mol Amine		mol CO <sub>2</sub> /mol Amine		mol CO <sub>2</sub> /mol Amine	
	Interface	Bulk	Interface	Bulk	Interface	Bulk
[PZ]	0.25	0.28	0.02	0.05	2.9E-4	1.8E-3
[PZCOO <sup>-</sup> ]	0.15	0.14	0.098	0.13	0.02	0.04
[PZ(COO <sup>-</sup> ) <sub>2</sub> ]	0.028	0.020	0.22	0.11	0.31	0.14
[MDEA]	3.67	3.69	2.92	3.18	1.00	1.42
Carbamate Approach to Equil. at Interface (%)	13	100	28	100	46	100
Dicarbamate Approach to Equil. at Interface (%)	14	100	40	100	86	100

\*All Concentrations presented in mol/L.  $P_{CO_2}^L/P_{CO_2}^* = 10$ ,  $k_1^o = 1.0E-4$  m/s.

driving force ( $10.0 * P_{CO_2}^*$ ) are considered. Also included are predictions of the pseudo-first-order enhancement factor, the enhancement factor predicted assuming global instantaneous reactions ( $E^{GLBL,INST}$ , Eq. 24), the enhancement factor predicted assuming all carbamate formation approaches instantaneous behavior ( $E^{PZ,INST}$ ), and the combined pseudo-first-order/PZ instantaneous enhancement factor ( $1/E^{PFO} + 1/E^{PZ,INST}$ ).  $E^{PZ,INST}$  is calculated by increasing all rate constants for carbamate formation until the enhancement factor approaches a steady value and will increase no more with increasing rate constant.

Table 6 demonstrates that, although the reaction of PZ with CO<sub>2</sub> is fast, it is not fast enough to be considered instantaneous. The behavior does, however, approach an instantaneous reaction with respect to the carbamate formation at high loading. Pseudo first order is also not a good assumption at higher loading. A simple addition of the pseudo first-order resistance and the PZ instantaneous resistance leads to a very accurate prediction of the enhancement factor with low driving force ( $1/E^{PFO} + 1/E^{PZ,INST}$ ).

Table 7 shows interfacial and bulk phase concentrations of PZ species at various loadings. At low loading ( $\alpha = 0.07$ ), it is easy to see that pseudo first order is a good approximation. There is not much depletion of PZ at the interface and there is still enough PZ around in the bulk solution. Examining the concentration of PZ carbamate, it is diffusing away from the interface, which makes it appear as a reaction product. The moderate loading ( $\alpha = 0.20$ ) demonstrates that there is beginning to be a significant amount of depletion of PZ at the

interface (about 60% depletion). Interestingly, the production of PZ carbamate from PZ under these conditions helps the depletion of carbamate to form dicarbamate. As a result, there is almost no depletion of PZ carbamate at the interface. At higher loading in region 3, we finally see some depletion of the MDEA. PZ is severely depleted, as well as PZ carbamate which has changed from being a reaction product in the region 1 to a reactant in region 3. There is also a steep gradient in dicarbamate at these conditions showing that much of the CO<sub>2</sub> is moving across the boundary layer in the form of dicarbamate.

We have also analyzed the concentration of mono and dicarbamate as a percentage of their equilibrium value. The carbamate formation reactions approach equilibrium at high loading, consistent with our observation that these reactions approach instantaneous behavior.

It is also useful to analyze the total amount of CO<sub>2</sub> being transferred across the boundary layer by different mechanisms. We define the total amount of carbamate and carbonate species respectively as

$$\begin{aligned}
 [\text{CARBAMATE}] &= [\text{PZCOO}^-] + [\text{H}^+ \text{PZCOO}^-] \\
 &\quad + 2[\text{PZ}(\text{COO}^-)_2] \\
 [\text{CARBONATE}] &= [\text{HCO}_3^-] + [\text{CO}_3^{2-}]
 \end{aligned}$$

At low loading, almost all the gradient in the total CO<sub>2</sub> species is in the form of carbamate species (99%). The same can be said about moderate loading where 94% of total CO<sub>2</sub>

**Table 8. Conditions for Ammonia Plant Example**

Parameter	Value	Notes
Temperature	313 K	Hefner et al. (1992)
Pressure	300 psi	Hefner et al. (1992)
Treated Gas CO <sub>2</sub> Conc.	0.05 vol. %	Typical Ammonia Plant
Inlet Gas CO <sub>2</sub> Conc.	18 vol. %	Typical Ammonia Plant
Lean Loading (mol CO <sub>2</sub> /mol Amine)	0.095	Calculated using VLE code factor of 3 from pinch
Rich Loading (mol CO <sub>2</sub> /mol Amine)	0.75	Calculated using VLE code factor of 3 from pinch
Ave. Molecular Wt.-Gas	16.11 g/mol	Hefner et al. (1992)
Mass Velocity (Gas)	2.55 kg/m <sup>2</sup> ·s	Hefner et al. (1992)
Mass Velocity (Liquid)	10.3 kg/m <sup>2</sup> ·s	Calculated from solvent rate
Packing Specific Area	170 m <sup>-1</sup>	IMTP#40 Wagner et al. (1997)
Calculated Wetted Area	132 m <sup>-1</sup>	Calculated per Onda et al. (1968)
Packing Particle Diameter	40 mm	Nominal Packing Diameter
$k_g$ (mol/(cm <sup>2</sup> ·atm·s))	1.19E-5	Calculated from Onda et al. (1968)
$k_1$ (cm/s)	3.04E-3	Calculated from Onda et al. (1968)

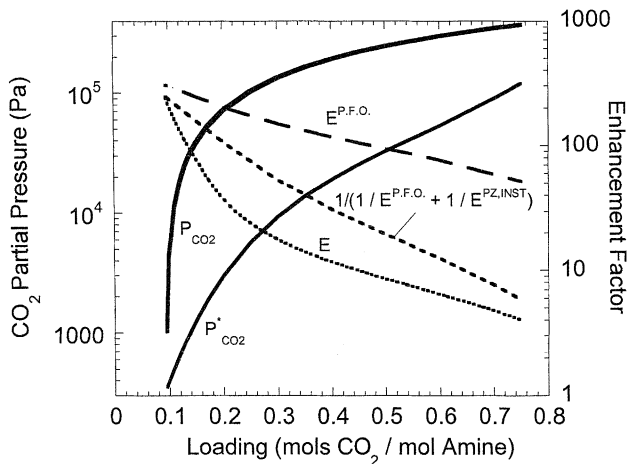


**Figure 7. McCabe Theiele diagram and enhancement factor prediction for ammonia plant case using rigorous model.**

40°C,  $P = 300$  psig,  $k_1^o = 3.0E-5$  m/s.

is being transferred as carbamate species. At high loading, however, only 66% of the total  $CO_2$  gradient is due to the carbamate species while 24% is due to molecular  $CO_2$  and the balance is due to the carbonate species.

### Ammonia Plants/Hydrogen Plants

We consider a typical ammonia or hydrogen plant scrubber and make model predictions at industrial conditions. Table 8 shows the conditions used in developing the example. Calculated parameters such as lean amine loading, mass-transfer coefficient calculated using the model of Onda et al. (1968) and other performance parameters are shown in Table 8. We have used a factor of three away from equilibrium at the lean and rich ends in order to define the solvent rate. Mathematically

$$P_{CO_2}^* @ \text{Top, Bottom} = \frac{P_{CO_2}}{3} @ \text{Top, Bottom} \quad (26)$$

Although we do not account for a temperature bulge in order to keep the example simple, the chosen solvent rate would still lie above the equilibrium curve for a bulge of 15°C at the bottom of the column. Figure 7 shows the operating line for this example and the corresponding isothermal equilibrium curve. The operating line may be as much as a factor of 30 deviated from the equilibrium curve at a loading of 0.20. Also shown on Figure 7 are the predicted and approximate enhancement factors according to Eq. 25 assuming instantaneous reactions for all carbamate formation. The approximate enhancement factors are quite accurate at the top and bottom, but have a significant deviation from the rigorous enhancement factors in the middle.

Using the enhancement factors generated above, we can calculate the height of a transfer unit and estimate the bed height for the isothermal case being studied. Although this is a simplification, the top of the column will approach isothermal behavior and we can gain insight into the dominant phys-

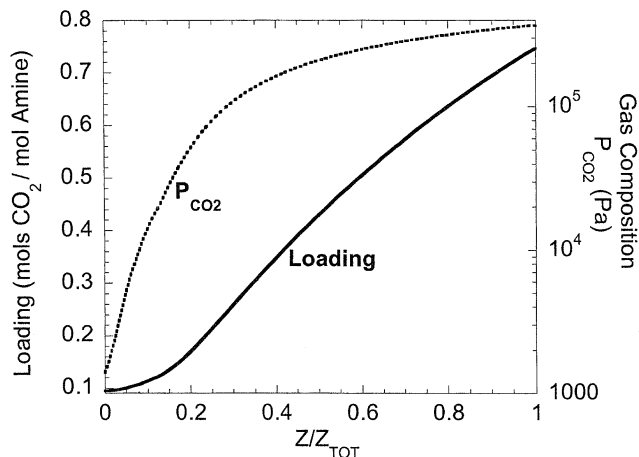


**Figure 8. Change in liquid and gas-phase compositions along column length for ammonia plant example using the rigorous model.**

40°C,  $P = 300$  psig,  $k_1^o = 3.0E-5$  m/s.

ical phenomenon at the top of the column. The total bed depth calculated was 65 ft, which is larger than expected yet reasonable. This is probably due to the fact that most plants would use a higher solvent rate to account for the temperature bulge and to reduce the rich loading. Figure 8 shows the loading and partial pressure as a function of bed depth. The mass transfer will be in a region of low loading ( $< 0.14$ ) for approximately the first 15% of the bed height. Moderate loading ( $0.14 < \alpha < 0.28$ ) is passed through quickly (at 30% of bed depth). The bulk of the column is at high loading. Figure 9 shows an overall gas phase transfer unit height and gas film resistance (%) as a function of bed depth. We define gas film control (%) as

$$\text{Resistance (\%)} = \frac{1/k_g}{1/K_G} \cdot 100 \quad (27)$$

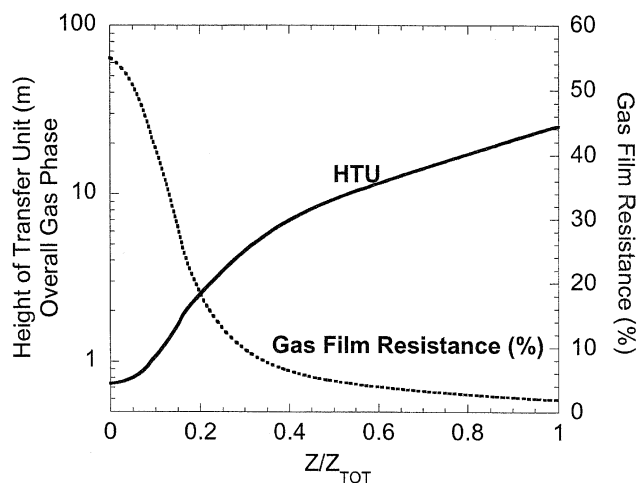


**Figure 9. Mass-transfer performance parameters for ammonia plant example using rigorous model.**

40°C,  $P = 300$  psig,  $k_1^o = 3.0E-5$  m/s.

The top of the column is 50% controlled by gas film resistance. The gas film resistance has reduced to 20% at a dimensionless bed depth of 0.2. The transfer unit curve distinctly shows the three regions. At dimensionless bed depths of less than 20%, the HTU curve has one slope that corresponds to low loading (<0.14). At bed depth above a dimensionless depth of 0.35 is a second slope that corresponds to high loading (>0.28) and is analogous to absorption into MDEA.

## Conclusions

### PZ/MDEA blend performance

5 wt. % PZ/45 wt. % MDEA provides almost two orders of magnitude and more enhancement than 50 wt. % MDEA at low loading and one order of magnitude enhancement at moderate loading. PZ/MDEA solvents outperform MEA/MDEA and DEA/MDEA blends at the same concentration.

### Approximate solutions

Pseudo first order is a good approximation to adsorption into PZ/MDEA blends at low loading, but not at moderate to high loading. At high loading, instantaneous carbamate formation is approached. A simplified model that combines the resistance of pseudo first-order reactions in series with instantaneous carbamate formation that matches the experimental data and rigorous model well.

### Important phenomena at different absorption conditions

The reaction of PZ to form monocarbamate is the dominant effect at low loading. At moderate loading, the dominant reaction is the reaction of monocarbamate to form dicarbamate. At high loading, the solution behaves like MDEA with instantaneous carbamate reactions.

Mass-transfer limitations due to gas-phase limitations are important at the top of an absorber in an ammonia plant. In some natural gas and flue-gas applications, gas-phase limitations would not be large due to slower liquid side enhancement caused by a higher lean loading and higher gas film mass-transfer coefficients due to lower pressure.

## Acknowledgments

This work was supported by the Separations Research Program at the University of Texas and other industrial sponsors.

## Notation

### Chemical Species

Symbol, Name, Formula

PZ = piperazine,  $C_4H_{10}N_2$   
 PZH<sup>+</sup> = protonated piperazine,  $C_4H_{11}N_2$   
 PZCOO<sup>-</sup> = piperazine carbamate,  $C_4H_{10}N_2COO^-$   
 PZ(COO<sup>-</sup>)<sub>2</sub> = piperazine dicarbamate,  $C_4H_9N_2(COO^-)_2$   
 H<sup>+</sup> PZCOO<sup>-</sup> = protonated piperazine carbamate,  $C_4H_{12}N_2COO^-$   
 MDEA = methyldiethanolamine,  $C_5H_{13}O_2N$   
 MDEAH<sup>+</sup> = protonated MDEA,  $C_5H_{14}O_2N$   
 CO<sub>2</sub> = carbon dioxide, CO<sub>2</sub>  
 HCO<sub>3</sub><sup>-</sup> = bicarbonate, HCO<sub>3</sub><sup>-</sup>

CO<sub>3</sub><sup>=</sup> = carbonate, CO<sub>3</sub><sup>=</sup>  
 H<sub>3</sub>O<sup>+</sup> = hydronium ion, H<sub>3</sub>O<sup>+</sup>  
 OH<sup>-</sup> = hydroxide ion, OH<sup>-</sup>  
 H<sub>2</sub>O = water, H<sub>2</sub>O

## Symbols

$D_i$  = diffusion coefficient of species  $i$   
 $E$  = true enhancement factor (both predicted and observed)  
 $E^{GLBL,INST}$  = enhancement factor assuming all reactions are instantaneous  
 $E^{PFO}$  = pseudo first-order enhancement factor  
 $E^{PZ,INST}$  = E. factor assuming only PZ and PZCOO<sup>-</sup>  $r \times ns$  to form carbamate are instantaneous  
 $H_{CO_2,H_2O}$  = Henry's constant for CO<sub>2</sub> in H<sub>2</sub>O  
 $H_{N_2O,H_2O}$  = Henry's constant for N<sub>2</sub>O in H<sub>2</sub>O  
 $k_{l,CO_2}$  = liquid film mass-transfer coefficient for CO<sub>2</sub>  
 $k_g$  = gas film mass-transfer coefficient  
 $K_G$  = overall mass-transfer coefficient, expressed using gas side  
 $k_{25}$  = rate constant at 25°C  
 $k_x$  = rate constant for reaction  $x$   
 $m$  = eddy diffusivity theory mass-transfer parameter—set to 2 in this work  
 $P_{CO_2}^*$  = equilibrium partial pressure of CO<sub>2</sub>  
 $P_{CO_2}$  = partial pressure of CO<sub>2</sub>  
 $R$  = universal gas constant  
 $r$  = liquid depth, dimensionless  
 $\mathcal{R}_i$  = overall rate of reaction for species  $i$   
 $T$  = temperature  
 $X$  = liquid depth measured from gas liquid interface  
 $-\Delta H_a$  = activation energy  
 $\epsilon$  = eddy diffusivity theory mass-transfer parameter  
 $\nabla$  = derivative operator  
 $\mu$  = liquid solution viscosity

## Literature Cited

- Al-Ghawas, H. A., D. P. Hagewiesche, G. Ruiz-Ibanez, and O. C. Sandall, "Physicochemical Properties Important for Carbon Dioxide Absorption in Aqueous Methyldiethanolamine," *J. Chem. Eng. Data*, **34**, 385 (1989).  
 Appl, M., U. Wagner, H. J. Henrici, K. Kuessner, F. Volkamer, and N. Ernst Neust, "Removal of CO<sub>2</sub> and/or H<sub>2</sub>S and/or COS From Gases Containing These Constituents," U.S. Patent No. 4336233 (1982).  
 Bishnoi, S., and G. T. Rochelle, "Absorption of Carbon Dioxide into Aqueous Piperazine: Reaction Kinetics, Solubility and Mass Transfer," *Chem. Eng. Sci.*, **55**, 5531 (2000).  
 Bishnoi, S., and G. T. Rochelle, "Thermodynamics of Piperazine/Methyldiethanolamine/Water/Carbon Dioxide," *Ind. Eng. Chem. Res.*, **41**, 604 (2002).  
 Bishnoi, S., "Carbon Dioxide Absorption and Solution Equilibrium in Piperazine Activated Methyldiethanolamine," PhD Diss., The University of Texas at Austin (2000).  
 Caplow, M., "Kinetics of Carbamate Formation and Breakdown," *J. Amer. Chem. Soc.*, **90**, 6795 (1968).  
 Chakravarty, T., U. K. Phukan, and R. H. Weiland, "Reaction of Acid Gas with Mixtures of Amines," *Chem. Eng. Prog.*, **91**, 32 (1995).  
 Critchfield, J. E., "CO<sub>2</sub> Absorption/Desorption in Methyldiethanolamine Solutions Promoted With Monoethanolamine and Diethanolamine: Mass Transfer and Reaction Kinetics," PhD Diss., The University of Texas at Austin (1988).  
 Danckwerts, P. V., "The Reaction of CO<sub>2</sub> with Ethanolamines," *Chem. Eng. Sci.*, **34**, 443 (1979).  
 Glasscock, D. A., and G. T. Rochelle, "Numerical Simulation of Theories for Gas Absorption with Chemical Reaction," *AIChE J.*, **35**, 8, 1271 (1989).  
 Glasscock, D. A., "Modelling and Experimental Study of Carbon Dioxide Absorption into Aqueous Alkanolamines," PhD Diss., The University of Texas, Austin (1990).  
 Glasscock, D. A., J. E. Critchfield, and G. T. Rochelle, "CO<sub>2</sub> Absorption/Desorption in Mixtures of Methyldiethanolamine with

- Monethanolamine and Diethanolamine," *Chem. Eng. Sci.*, **46**, 2829 (1991).
- Hefner, W., H. Meissner, and J. Davis, "Revamping of CO<sub>2</sub> Removal Systems by Activated MDEA Process," AIChE Symp., San Antonio, TX (Sept. 27–30, 1992).
- Kaganol, S., "Carbon Dioxide Absorption in Methyldiethanolamine with Piperazine or Diethanolamine: Thermodynamics and Rate Measurements," MS Thesis, The University of Texas at Austin (1997).
- Lewis, W. K., and W. G. Whitman, "Principles of Gas Absorption," *Ind. Eng. Chem.*, **16**, 12 (1924).
- Littel, R. J., "Selective Carbonyl Sulfide Removal in Acid Gas Treating Processes," PhD Diss., Twente University, The Netherlands (1991).
- Littel, R. J., G. F. Versteeg, and W. P. M. Van Swaaij, "Kinetics of CO<sub>2</sub> with Primary and Secondary Amines in Aqueous Solutions: II. Influence of Temperature on Zwitterion Formation and Deprotonation Rates," *Chem. Eng. Sci.*, **47**, 2037 (1992).
- Liu, J., G. Pope, and K. Sepehrnoori, "A High Resolution Finite Difference Scheme for Non-uniform Grids," *Appl. Math. Modelling*, **19**, 162 (1995).
- Liu, H.-B., C.-F. Zhang, and G.-W. Xu, "A Study on Equilibrium Solubility for Carbon Dioxide in Methyldiethanolamine-Piperazine-Water Solution," *Ind. Eng. Chem. Res.*, **38**, 4032 (1999).
- Onda, K., H. Takeuchi, and Y. Okumoto, "Mass Transfer Coefficients between Gas and Liquid Phases in Packed Columns," *J. of Chem. Eng. of Japan*, **56**, 1 (1968).
- Pacheco, M. A., "Mass Transfer Kinetics and Rate-Based Modeling of Reactive Absorption," PhD Diss., The University of Texas at Austin (1998).
- Prasher, B. D., and A. L. Fricke, "Mass Transfer at a Free Gas Liquid Interface in Turbulent Thin Films," *Ind. Eng. Chem. Process Des. Dev.*, **13**, 4, 336 (1974).
- Pinsent, B. R., L. Pearson, and F. J. W. Roughton, "The Kinetics of Combination of Carbon Dioxide with Hydroxide Ions," *Trans. Faraday Soc.*, **52**, 1512 (1956).
- Rowley, R. L., "Diffusion Coefficients in Aqueous Alkanolamines," GRI/GPA Research Report RR-163, GPA Project 911, GRI Contract No. 5092-260-2356 (1999).
- Toman, J. J., Draft PhD Diss., The University of Texas at Austin (1990).
- Versteeg, G. F., "Mass Transfer and Chemical Reaction Kinetics in Acid Gas Treating Processes," PhD Diss., Twente University, The Netherlands (1987).
- Wagner, I., J. Stichlmair, and J. R. Fair, "Mass Transfer in Beds of Modern, High Efficiency Random Packings," *Ind. Eng. Chem. Res.*, **36**, 227 (1997).
- Wammes, W., H. Meissner, and W. Hefner, "Activated MDEA Process: A Flexible Process for Acid Gas Removal from Natural Gas," Conference Preprint, Annual GPA Convention, New Orleans, LA (Mar. 7–9, 1994).
- Xu, G.-W., C.-F. Zhang, S.-J. Qin, and Y.-W. Wang, "Kinetics Study on Absorption of Carbon Dioxide into Solutions of Activated Methyldiethanolamine," *Ind. Eng. Chem. Res.*, **31**, 921 (1992).
- Xu, G.-W., C.-F. Zhang, S.-J. Qin, W.-H. Gao, and H.-B. Liu, "Gas-Liquid Equilibrium in a CO<sub>2</sub>-MDEA-H<sub>2</sub>O System and the Effect of Piperazine on It," *Ind. Eng. Chem. Res.*, **37**, 1473 (1998).

Manuscript received Aug. 22, 2001, and revision received Apr. 10, 2002.